Research article

Rapports De Pharmacie Vol.3 (3), 2017, 395-407
ISSN: 2455-0507

DESIGN, OPTIMIZATION AND CHARACTERIZATION OF AZILSARTAN NANOPARTICLES USING DESIGN-EXPERT® SOFTWARE VERSION 11

Tai Yee Ling, Jaya Raja Kumar

[1]*Research student, Asian Institute of Medicine, Science and Technology (AIMST) University, Bedong 08100, Kedah, Malaysia*

[2]*Unit of Pharmaceutical Technology, Faculty of Pharmacy, Asian Institute of Medicine, Science and Technology (AIMST) University, Bedong 08100, Kedah, Malaysia*

ABSTRACT

In this work, the purpose of the study was to formulate and optimize azilsartan nanoparticles by employing factorial design. The nanoparticles were prepared successfully with a modified emulsification method by using biodegradable and biocompatible polymer poly (L-lactide) (PLA). Various process parameters were manipulated to investigate their effects on particle size, polydispersity index, entrapment efficiency and percentage of cumulative drug release after 12 hours of formulated nanoparticles. In addition, morphology and compatibility between the drug and polymer of nanoparticles were studied with scanning electron microscope (SEM) and FTIR studies. The optimized formulation had a particle size range of 267.14 - 280.01 nm, PDI range of 0.101-0.361, entrapment efficiency range of 69.14 - 84.72% and % CDR after 12 hours 56.11 - 67.01%. The nanoparticles were confirmed to be spherical in shape by SEM results while FTIR results established the compatibility of components of the formulation.

Keywords: Azilsartan, Nanoparticles, Polylactic acid, Box-Cox Plot, HPLC

INTRODUCTION

While hypertension is one of the major problems affecting most populations of the world, it remains still not adequately controlled despite the existence of various anti-hypertensive medications. Among all the anti-hypertensive medications, the drugs that act by modulating renin-angiotensin-aldosterone system (RAAS) are proved for their efficacy and commonly used in management of hypertension. Azilsartan is classified as angiotensin receptor blocker (ARB) which exhibits its efficacy by binding directly to angiotensin type 1 (AT_1) receptors.[1] Azilsartan is also being referred as TAK-536 and its IUPAC name is 2-ethoxy-1-{[2'-(5-oxo-4,5-dihydro-1,2,4-oxadiazol-3-yl)biphenyl-4-yl]methyl} -1H-benzimidazole-7-carboxylic acid. The chemical structure of azilsartan is shown in Figure 1.[2] Azilsartan was approved by US Food and Drug Administration (FDA) in 2011 to control hypertension in adults. Azilsartan has a high affinity to AT_1 receptors for prolonged period. When it occupies AT_1 receptors, angiotensin II is unable to bind to AT_1 receptors, hence the action of angiotensin II is blocked. Since angiotensin II is a potent vasoconstrictor and it can stimulate the secretion of aldosterone, when angiotensin II action is inhibited, vasoconstriction and aldosterone effects are also inhibited. Consequently, blood pressure reduces. The efficacy of azilsartan is found excellent than valsartan and olmesartan.[3] As hypertension is associated with higher risks of complications such as stroke, heart failure, myocardial infarction and other end organ damage, hypertension must be controlled well.[4] Intensive treatment is needed for patients not achieving the target goal of blood pressure. In order to achieve better therapeutic outcome in patients taking azilsartan, a targeted and controlled release formulation of azilsartan was studied and developed in this paper as nanoparticle formulation.

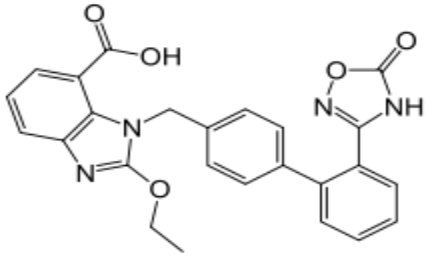

Figure-1: Structure of Azilsartan.

In view of the rapid evolution of nanomedicine in near decades, nanoparticles have established their potential to provide targeted drug delivery. This plays a significance impact in medicines as dose of a particular drug can be reduced for minimal side effects with targeted drug delivery. Nanoparticles would circulate in the body until they reach their specific targets where they selectively accumulate to exhibit the drug action encapsulated in the

Address for correspondence:
Tai Yee Ling,
Research student,
AIMST University,Bedong- Semeling, Kedah, Malaysia- 08100

nanoparticles.[5] When nanoparticles circulate in body and contact with various biological materials such as blood, proteins and other molecules found in the environment would attached to the surface of the nanoparticles and form layers around nanoparticles naturally. These layers are known as biocorona. Biocorona has a significance impact on the actions of nanoparticles because different biocorona will render the nanoparticles distinct chemical properties, distribution, elimination and reactions with the body even the nanoparticles are of same types, giving the nanoparticles distinct biological identities.[6] This is supported by recent study showing that cells are suggested to recognize distinct populations of nanoparticles with distinct biological identities.[7] A polymeric nanoparticle formulation can be developed by using a polymer such as polylactic acid, chitosan, PLGA, poly-caprolactone and poly-alkylcyanoacrylate.[8] These polymeric nanoparticles even enhance the therapeutic efficacy of nanoparticle formulations by providing controlled and sustained release of drug. As different methods and polymers utilized during the production of nanoparticles formulation, the performance of the resultant nanoparticles would also vary. Therefore, while azilsartan is the drug of investigation in this study, we would like to study the characteristics of azilsartan nanoparticles formulated with polylactic acid (PLA).

Polylactic acid is a lipophilic and biodegradable polymer. Lactic acid, the constituting monomer, is easily derived from renewable resources like corn starch or sugarcane. The fact that lactic acid is the only degradation product following the polymer hydrolysis makes PLA polymer of interest for several applications. In medicine, it is used to produce bioabsorbable implants for orthopaedic surgery, for the treatment of facial lipoatrophy in HIV patients as well as for treatment of scars and for esthetic rejuvenation. PLA micro- and nano-particles have widely been studied as delivery systems for systemic and topical applications.[9] Poly-lactic acid nanoparticles (PLA-NP) exhibit their potential applications in nanomedicine as carriers of drugs, genes, proteins and many other therapeutic agents, owing to its lipophilicity, biodegradability, biocompatibility, low toxicity, strong mechanical strength and slow drug release.[10] As a polymeric nanoparticles, PLA-NP provides sustained release of drug encapsulated where the drug release kinetics can be controlled by polymer matrix of PLA-NP. In fact, PLA have been approved to be used in human by FDA after the evaluation of PLA cytotoxicity in various studies involving distinct cell types such as CHO-K1, HEK293 and retinal pigment epithelium. These studies concluded that PLA-NP were non-cytotoxic; these conclusions were based on the assessment of cell viability through measurements of mitochondrial activity, while other cellular stress parameters were not considered.[11]

The aim of this study was to formulate and optimize azilsartan nanoparticles with PLA using a factorial design. An experimental Box-Behnken design was used to evaluate the influence of sonication time to obtain the emulsion, proportion of azilsartan and PLA in the properties of resultant azilsartan nanopartilces.

MATERIALS AND METHODS

Materials:

Azilsartan obtained from Sigma-Aldrich Co., Poly(L-lactide) obtained from Sigma-Aldrich Co., Polyvinyl alcohol obtained from R&M Marketing, Essex, U.K., Dichloromethane obtained from ACI Labscan, Acetone obtained from EMSURE, Potassium bromide obtained from Nacalai Tesque, distilled water and deionised water from MDL-4 Lab, AIMST University. All other materials and chemicals were of analytical grade.

Methods:

Preparation of Azilsartan nanoparticles:

Azilsartan nanoparticles were prepared by using different proportions of drug and polymers and sonication time. The polymer used in this preparation of nanoparticles was polylactic acid (PLA) while the aqueous phase was 1% w/v polyvinyl alcohol (PVA). In the preparation, accurately weighed azilsartan was first dissolved in acetone. PLA was mixed with 1.5 ml of dichloromethane (DCM) and then mixed thoroughly in drug solution. This dispersed phase containing azilsartan and PLA was added drop wise to PVA solution and sonicated for definite time using (Qsonica Q55 Sonicator, USA). It was followed with magnetic stirrer with rotation speed 1000 rpm at 70^{o}C for 1 hour. To separate the nanoparticles from the continuous phase and residual solvent, first, azilsartan-PLA nanoparticles were centrifuged (Beckman Coulter Avanti J-26S XPI centrifuges) and the supernatant was discarded. The NPs were washed 2 times. Finally, the sample was lyophilized (Thermo Scientific-SuperModulyo 230, USA).

Determination of Particle Size and Polydispersity Index:

The samples of azilsartan nanoparticles were diluted with water (Viscosity 0.8903 mPa.S) for

determination of particle size and polydispersity index by using Anton Paar Malaysia - Litesizer 500. Each measurement were done in triplicate.[12]

Determination of entrapment efficiency:

10ml of azilsartan nanoparticles solution was subjected for centrifugation at 5000rpm for 20 min. The supernatant solution was then filtered. 1ml of the filtrate was diluted with water, followed with measurement of entrapment efficiency by using HPLC method. The amount of free drug in the sample was determined and the percentage of entrapment efficiency was calculated from the following equation.[13]

Percentage of entrapment efficiency = $\frac{total\ drug\ in\ formula - free\ drug}{total\ drug\ in\ formula} \times 100\%$

In-vitro drug release:

Percentage of cumulative drug release of azilsartan nanoparticles was obtained from dissolution study of nanoparticles. The dissolution study was performed by using Electrolab's dissolution testers (USP) at 50 rpm with 900 ml of phosphate buffer 7.4 as dissolution medium which maintained at a temperature of 37°C ± 0.5°C.

At predetermined time intervals, 2 mL release medium was taken out from flask and replaced with 2 mL fresh phosphate buffer to keep the volume constant. The concentration of drug in the medium was determined by using HPLC method. Subsequently, the percentage of cumulative drug released was obtained after 12 hours.[14]

RP HPLC chromatographic separation was performed on a Shimadzu liquid chromatographic system equipped with a LC-20AD solvent delivery system (pump), SPD-20A photo diode array detector, and SIL-20ACHT injector with 50µL loop volume. The LC solution version 1.25 was used for data collecting and processing (Shimadzu, Japan). The HPLC was carried out at a flow rate of 1.0 ml/min using a mobile that is phase constituted of acetonitrile, 0.5% TEA: ACN (pH 4.5) (40:60, v/v), and detection was made at 248nm. The mobile phase was prepared daily, filtered through a 0.45µm membrane filter (Millipore) and sonicated before use. A Thermo C18 column (25cm × 4.6mm i.d., 5µ) was used for the separation.

Fourier transforms Infrared spectroscopy:

FT-IR study of azilsartan and physical mixture of azilsartan and PLA were performed to identify any interaction or incompatibility between the drug and polymer used. FT-IR spectra of Azilsartan and physical mixture of azilsartan with PLA were performed employing KBr pellet technique at room temperature. The IR spectra were recorded using Perkin Elmer Spectrum GX FT-IR, measured over a range 4000-400 cm^{-1}.[15]

RESULTS AND DISCUSSION

Experimental Design:

This paper summarized the successful effect on the formulation of azilsartan loaded PLA nanoparticles. Through preliminary experiments, Azilsartan (A), PLA (B) and Sonication Time (C) were identified as the most significant variables influence the particle size, PDI, Entrapment efficiency, and percentage of CDR after 12 hours. Among various design approaches, the Box-Behnken (BBD) has good and reliable design properties as shown in table 1.

Seventeen runs were performed for response surface methodology (RSM) based on the box-behnken design. Based on the experimental design, the factor combinations produced different responses as presented in Table 2. These results clearly indicated that all the dependent variables were strongly dependent on the selected independent variables as they showed a wide variation among the 17 runs in Table 3. Stat-Ease's Design-Expert® software, version 11 was used for analysis of variance (ANOVA), regression coefficients and regression equation. Mathematical relationship generated using the equation in terms of coded factors can be used to make predictions about the response for given levels of each factor as shown in Table 4.

Table-1: Build Information.

File Version	**11.0.4.0**		
Study Type	Response Surface	Subtype	Randomized
Design Type	Box-Behnken	Runs	17
Design Model	Quadratic	Blocks	No Blocks
Build Time (ms)	2.00		

Table-2: List of Independent variable and Dependent variables in Box-Behnken design.

Independent variable			Levels		
Variable	Name	Units	Low	Middle	High
A	Azilsartan	mg	20	30	40
B	PLA	mg	50	75	100
C	Sonication Time	min	5.0	7.5	10.0
Dependent variable				**Goal**	
R1	Particle size	nm		Minimize	
R2	Polydispersity index	-		Moderate	
R3	Entrapment efficiency	%		Maximize	
R4	Cumulative drug release	%		Moderate	

Table-3: Factorial design of azilsartan loaded PLA nanoparticles.

Run	A:Azilsartan(mg)	B:PLA (mg)	C:Sonication Time (min)	Particle size (nm)	Polydispersity index	% of Entrapment efficiency	% CDR after 12 hours
1	30	50	5	276.05	0.122	71.47	59.17
2	20	75	10	267.41	0.179	71.52	58.51
3	30	75	7.5	270.36	0.103	79.46	58.56
4	40	75	5	267.48	0.154	79.99	65.11
5	20	100	7.5	269.99	0.268	84.72	66.57
6	20	75	5	269.21	0.156	84.11	65.16
7	20	50	7.5	267.14	0.361	81.76	59.98
8	40	75	10	280.01	0.261	79.14	56.87
9	40	50	7.5	279.07	0.266	72.37	56.11
10	30	50	10	274.11	0.127	69.14	56.41
11	30	75	7.5	271.96	0.103	79.38	58.14
12	40	100	7.5	269.47	0.281	81.44	67.01
13	30	75	7.5	270.06	0.101	79.85	58.68
14	30	100	10	277.22	0.241	82.31	66.11
15	30	75	7.5	271.02	0.102	79.12	58.61
16	30	75	7.5	270.15	0.102	79.41	58.77
17	30	100	5	274.14	0.275	83.72	65.32

Table-4: Regression equation for the response.

Response Regression equation
Particle size = $+270.71+2.79A-0.6937B+1.48C-3.11AB+3.58AC+1.26BC-1.82A^2+2.53B^2+2.14C^2$
Polydispersity index = $+0.1022-0.0002A+0.0236B+0.0126C+0.0270AB+0.0210AC- 0.0098BC+0.0940A^2+ 0.0978B^2-0.0087C^2$
Entrapment efficiency = $+78.76-1.15A+4.68B-2.15C$
% CDR after 12 hour = $+58.55-0.6400A+4.17B-2.11C+1.08AB-3975AC+0.8875BC+1.76A^2+2.10B^2+1.10C^2$

Table-5: ANOVA results of the quadratic model for the response particle size (R1).

Source	Sum of Squares	DF	Mean Square	F-value	p-value	R^2
Model	239.02	9	26.56	8.47	0.0051	0.9159
A-Azilsartan	62.05	1	62.05	19.79	0.0030	
B-PLA	3.85	1	3.85	1.23	0.3044	
C-sonication time	17.61	1	17.61	5.62	0.0496	
AB	38.75	1	38.75	12.36	0.0098	
AC	51.34	1	51.34	16.37	0.0049	
BC	6.30	1	6.30	2.01	0.1993	
A^2	13.99	1	13.99	4.46	0.0726	
B^2	26.95	1	26.95	8.59	0.0220	
C^2	19.28	1	19.28	6.15	0.0422	
Residual	21.95	7	3.14			
Lack of Fit	19.43	3	6.48	10.29	0.0237	

Table-6: ANOVA results of the quadratic model for the response polydispersity index (R2).

Source	Sum of Squares	DF	Mean Square	F-value	p-value	R^2
Model	0.0926	9	0.0103	3.38	0.0613	0.8128
A-Azilsartan	5.000E-07	1	5.000E-07	0.0002	0.9901	
B-PLA	0.0045	1	0.0045	1.47	0.2653	
C-sonication time	0.0013	1	0.0013	0.4186	0.5383	
AB	0.0029	1	0.0029	0.9573	0.3605	
AC	0.0018	1	0.0018	0.5791	0.4715	
BC	0.0004	1	0.0004	0.1248	0.7342	
A^2	0.0372	1	0.0372	12.22	0.0100	
B^2	0.0403	1	0.0403	13.22	0.0083	
C^2	0.0003	1	0.0003	0.1052	0.7551	
Residual	0.0213	7	0.0030			
Lack of Fit	0.0213	3	0.0071	10151.79	<0.0001	

Particle size analysis of azilsartan nanoparticles was found to be in the range of 267.14 - 280.01 nm as shown in Table 3. The Model F-value of 8.47 implied the significance of the model. There was only 0.51% chance that an F-value this large could occur due to noise. Values of "P-values" less than 0.0500 indicated the model terms were significant. In this case A, C, AB, AC, B^2, C^2 were significant model terms. The "Lack of Fit F-value" of 10.29 implied there was a 2.37% chance that a "Lack of Fit F- value" this large could occur due to noise.

The coefficient of determination R^2 measured the fraction of the total squared error that was explained by the model. The range of R^2 lied between 0 and 1. The closer the R^2 value to 1, the better the result but a large value of R^2 value did not necessarily indicate a good regression model. Whenever a variable was added to the model, regardless of whether the added variable was significant statistically or not, it will always increase the R^2. Therefore, the models might have large values of R^2 poor predictions of new observations or estimates of the mean response. In order to avoid this misinterpretation, the Adjusted R^2 statistic which values would decrease when insignificant terms were added into the models can be added in the analysis. These two statistics were able to imply the presence of extraneous terms in the computed model, indicated by a large difference between the two statistical values, usually of greater than 0.20. On the other hand, the difference between the predicted output by the model and the actual output was known as residual while Predicted Residual Error Sum of Squares (PRESS) measured how the model fitted each point in the design and was used to calculate predicted R^2.

Here, the "Predicted R^2-value" was -0.2065 and the "Adjusted R^2-value" was 0.8077. "Adeq Precision" measured the signal to noise ratio where a ratio greater than 4 is desirable. As we obtained a ratio of

9.377, it indicated an adequate signal and this model capable of navigating the design space.

The normality of the data could be investigated through the normal % probability plot of the externally studentized residuals as shown in Figure 2. Residuals vs. Run were scattered randomly between the outlier detection limits +4.81 to -4.81 as shown in Figure 3. Value of $\lambda = 1.00$ indicates that no transformation was needed and was able to produce identical results to original data shown in Figure 4. Cook's distance vs. Run are also analysed as shown in Figure 5. The relationship between the modifiable and dependent variables was elucidated using 3D response surfaces in Figure 6(a). The shapes of response surfaces and contour plots reveal the nature and extent of the interaction between different factors. The particle size distribution of azilsartan nanoparticles was shown in Figure 6(b). At low levels of A (Drug), R1 obtained from 267.14 to 269.99 nm. Similarly at high levels of A, R1 obtained from 267.48 to 280.01 nm.

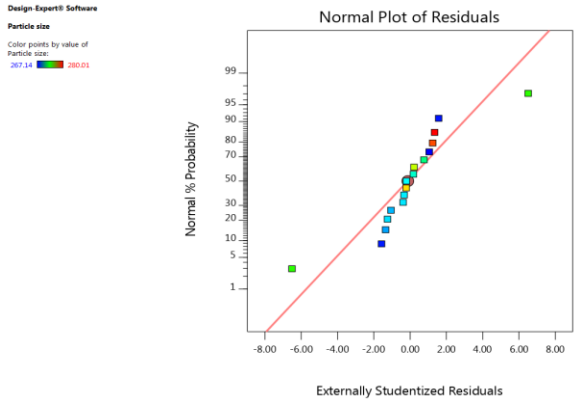

Figure-2: Normal % probability plot of the externally studentized residuals (R1).

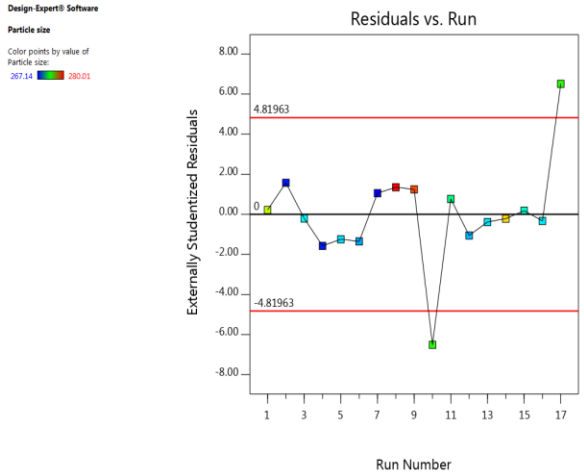

Figure-3: Residuals vs. Run (R1).

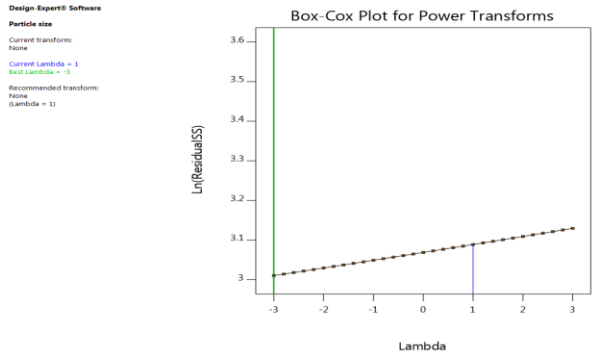

Figure-4: Box-Cox Plot for Power Transforms (R1).

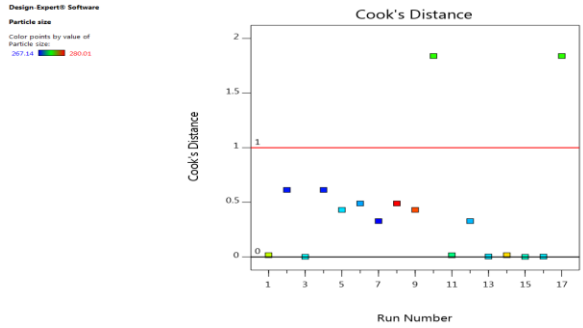

Figure-5: Cook's Distance vs. Run (R1).

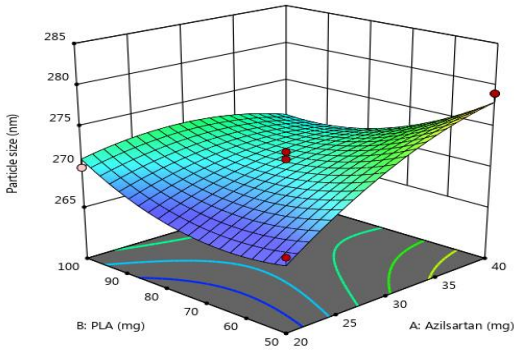

Figure-6(a): Response surface plot presenting the interaction between the drug and PLA affecting the particle size (R1).

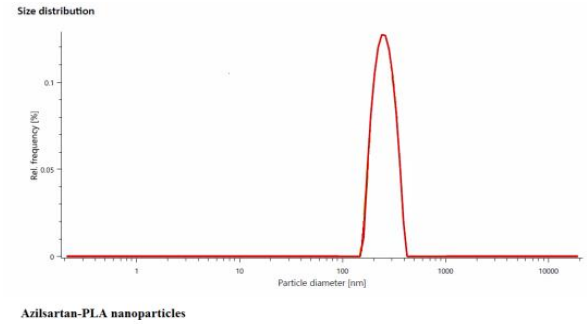

Figure-6(b): Particle size distribution of azilsartan nanoparticles.

Polydispersity index analysis of azilsartan nanoparticles was found to be in the range of 0.101-0.361 as indicated in Table 3. The Model F-value of 3.38 implied a 6.13 % chance that an F-value this large could happen due to noise. A^2 and B^2 is significant model terms in this case as they have a "P-values" less than 0.0500 where other model terms with "P-values" greater than 0.1000 were not significant. Model reduction may improve the model if there were many insignificant model terms in the study. The "Lack of Fit F-value" of 10151.79 implied the Lack of Fit was significant. There is a 0.01% chance that a "Lack of Fit F-value" this large could occur due to noise. The "Predicted R^2-value" is -1.9944 and the "Adjusted R^2 –value" is 0.5722. The overall mean may be a better predictor of the response than the current model when a negative "Predicted R^2" was obtained. An "Adeq Precision" ratio of 5.7213 indicates an adequate signal and this model can be used to direct the design space.

As similar to R1, the normality of the data could be proved through the normal % probability plot of the externally studentized residuals. The points on the plot lied on a straight line; the residuals were normally distributed as confirmed in Figure 7. The points in Residuals vs. Run scattered randomly between the outlier detection limits +4.81 to -4.81 in Figure 8.Value of $\lambda = 1.00$ indicates that no transformation needed and produced results identical to original data shown in Figure 9. Cook's distance vs. Run and the influence of the main and interactive effects of A, B and C on polydispersity index (R2) of Azilsartan nanoparticles was further elucidated using 3D response surfaces as shown in Figure 10 and Figure 11 respectively. At low levels of A (Drug), R2 obtained from 0.156 to 0.361. At high levels of A, R2 was obtained from 0.154 to 0.281.

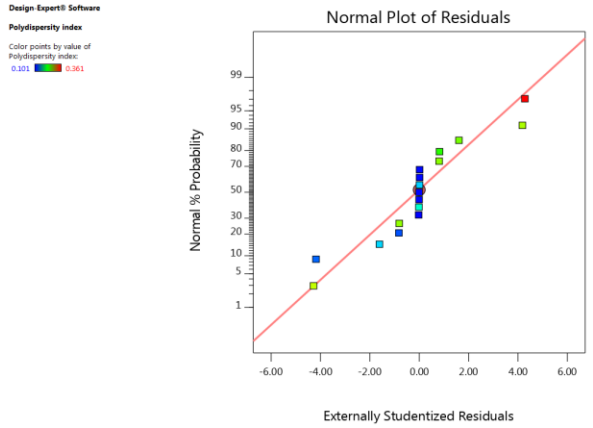

Figure-7: Normal % probability plot of the externally studentized residuals (R2).

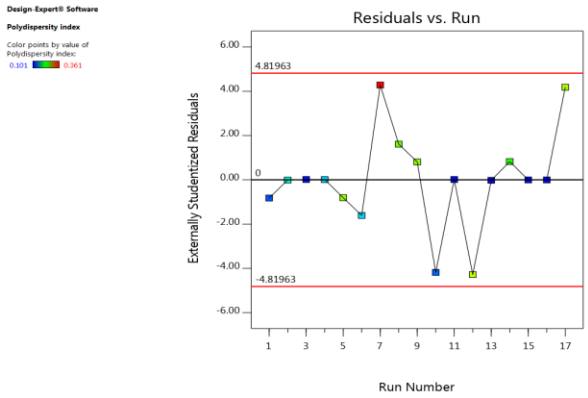

Figure-8: Residuals vs. Run (R2).

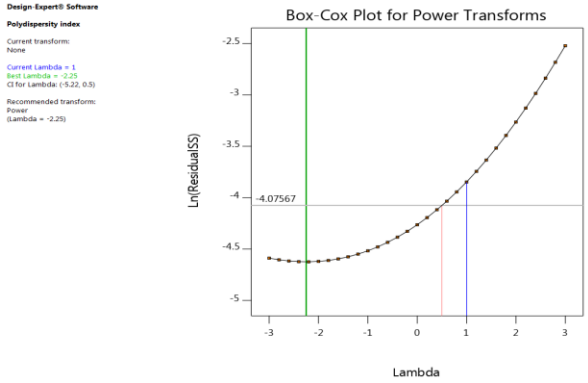

Figure-9: Box-Cox Plot for Power Transforms (R2).

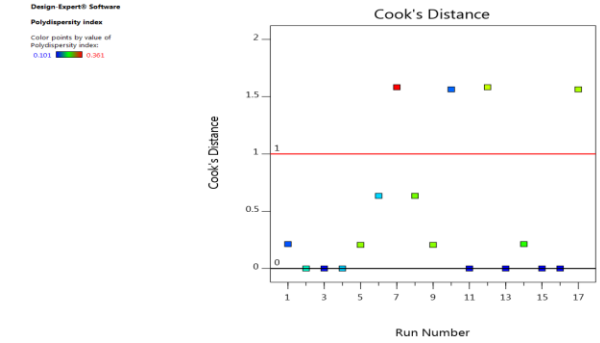

Figure-10: Cook's Distance vs. Run (R2).

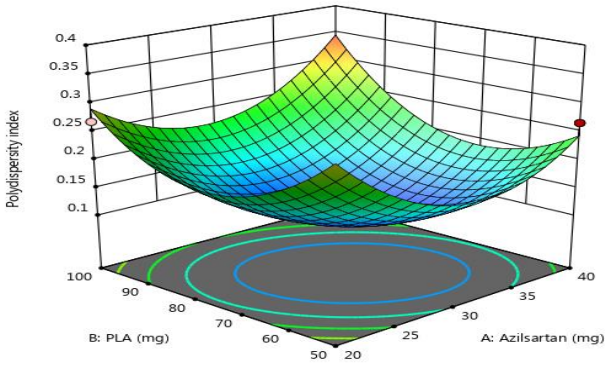

Figure-11: Response surface plot presenting the interaction between the drug and PLA affecting the polydispersity index (R2).

Entrapment efficiency analysis of azilsartan nanoparticles was found to be in the range of 69.14 - 84.72%. The Model F-value of 6.99 implied the significance of the model with only a 0.48% chance that an F-value this large could occur due to noise. Values of "P-values" less than 0.0500 indicated the model terms were significant but only B was a significant model term in this case as shown in Table 9. The "Lack of Fit F-value" of 222.36 implied the Lack of Fit was significant and there was only a 0.01% chance that a "Lack of Fit F- value" this large could occur due to noise. The "Predicted R^2-value" was 0.2061 and the "Adjusted R^2-value" was 0.5291. The difference was more than 0.2, indicating the possibility of a large block effect or problem with the model or data where model reduction, response transformation, outliers, etc. should be considered. "Adeq Precision" of 8.6410 was obtained. Since a ratio greater than 4 was preferred, this indicated an adequate signal for this model to be used to navigate the design space.

The normality of the data was investigated through the normal % probability plot of the externally studentized residuals in Figure 12. Residuals vs. Run were scattered randomly between the outlier detection limits +3.71 to -3.71 as shown in Figure 13. Box-Cox Plot for Power Transforms gave a value of $\lambda = 1.00$ indicated that no transformation was needed and produced results identical to original data in Figure 14. Cook's distance vs. Run was analysed and the influence of the main and interactive effects of A, B and C on the entrapment efficiency (R3) of azilsartan nanoparticles was further elucidated using 3D response surfaces as shown in Figure 15 and Figure 16 respectively. At low levels of A (Drug), R3 increased from 71.52% to 84.72%. At high levels of A, R3 increased from 72.37% to 81.44%.

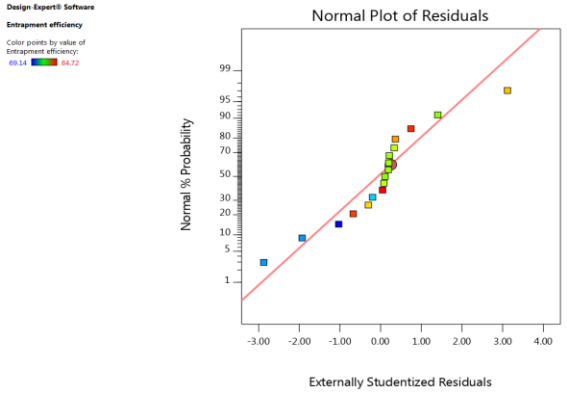

Figure-12: Normal % probability plot of the externally studentized residuals (R3).

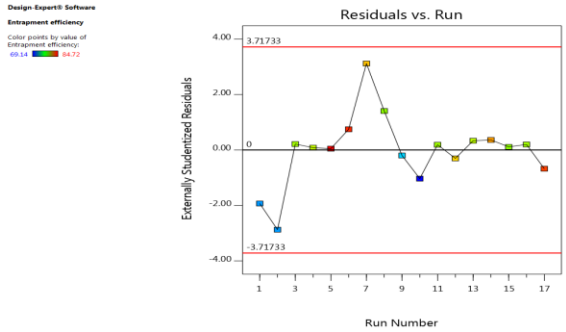

Figure-13: Residuals vs. Run (R3).

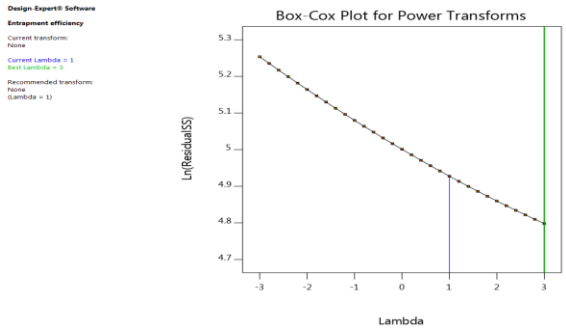

Figure-14: Box-Cox Plot for Power Transforms (R3).

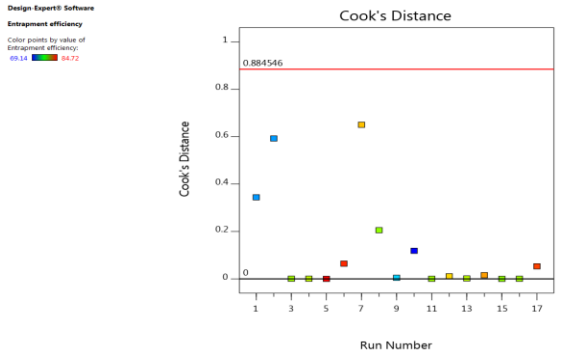

Figure-15: Cook's Distance vs. Run (R3).

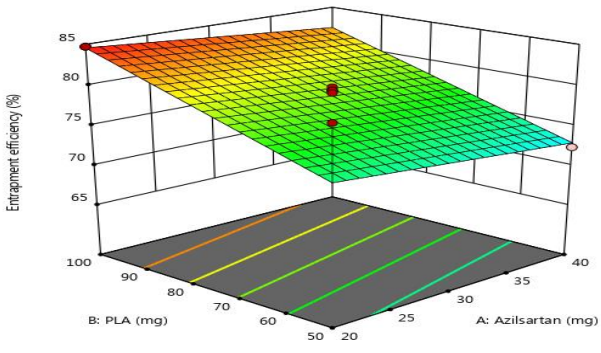

Figure-16: Response surface plot presenting the interaction between the drug and PLA affecting the entrapment efficiency (R3).

Table-7: ANOVA results of the quadratic model for the response entrapment efficiency (R3).

Source	Sum of Squares	DF	Mean Square	F-value	p-value	R^2
Model	222.72	3	74.24	6.99	0.0048	0.6174
A-Azilsartan	10.51	1	10.51	0.9900	0.3379	
B-PLA	175.31	1	175.31	16.51	0.0013	
C-sonication time	36.89	1	36.89	3.47	0.0850	
Residual	138.02	13	10.62			
Lack of Fit	137.75		15.31	222.36	<0.0001	

Table-8: ANOVA results of the quadratic model for the response percentage of CDR after 12 hour (R4).

Source	Sum of Squares	DF	Mean Square	F-value	p-value	R^2
Model	226.91	9	25.21	8.09	0.0058	0.9123
A-Azilsartan	3.28	1	3.28	1.05	0.3393	
B-PLA	138.94	1	138.94	44.58	0.0003	
C-sonication time	35.53	1	35.53	11.40	0.0118	
AB	4.64	1	4.64	1.49	0.2617	
AC	0.6320	1	0.6320	0.2028	0.6661	
BC	3.15	1	3.15	1.01	0.3482	
A^2	13.08	1	13.08	4.20	0.0797	
B^2	18.62	1	18.62	5.97	0.0445	
C^2	5.07	1	5.07	1.63	0.2427	
Residual	21.82	7	3.12			
Lack of Fit	21.58	3	7.19	121.37	0.0002	

Percentage of CDR after 12 hour analysis of azilsartan nanoparticles was found to be in the range of 56.11 - 67.01% as indicated in Table 3. The Model F-value of 8.09 implies the model was significant with only a 0.58% chance that an F-value this large could occur due to noise. B, C, B^2 were having "P-values" less than 0.0500, indicating them as the significant model terms in this case. The "Lack of Fit F-value" of 121.37 implied the Lack of Fit was significant and there is only a 0.02% chance that a "Lack of Fit F- value" this large could occur due to noise. The "Predicted R^2 value was -0.3897 and adjusted R^2 value was 0.5291. "Adeq Precision" with ratio greater than 4 was looked-for and our ratio of 9.269 showed an adequate signal to navigate the design space.

The normality of the data and Cook's distance vs. Run were analysed in Figure 17 and Figure 20. Normality of the data could be proved through the normal % probability plot of the externally studentized residuals. Residuals vs. Run showed the points were scattered randomly between the outlier detection limits +4.81 to -4.81 as shown in Figure 18.Value of $\lambda = 1.00$ Box-Cox Plot for Power Transforms indicated that no transformation needed and produced identical results to original data as shown in Figure 19. The relationship between the variables was further demonstrated using 3D response surfaces as shown in Figure 21. At low levels of A (Drug), R4 obtained from 58.51% to 66.57%. At high levels of A, R4 increases from 56.11% to 67.01%.

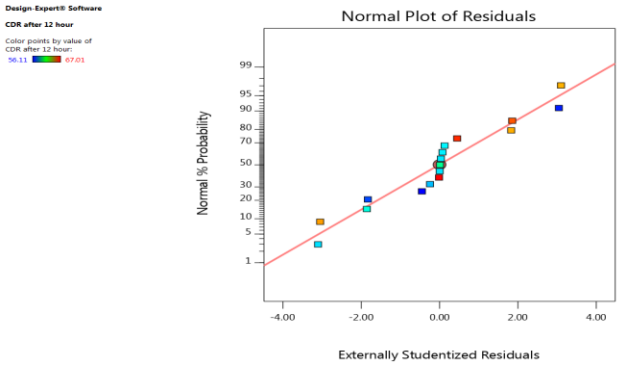

Figure-17: Normal % probability plot of the externally studentized residuals (R4).

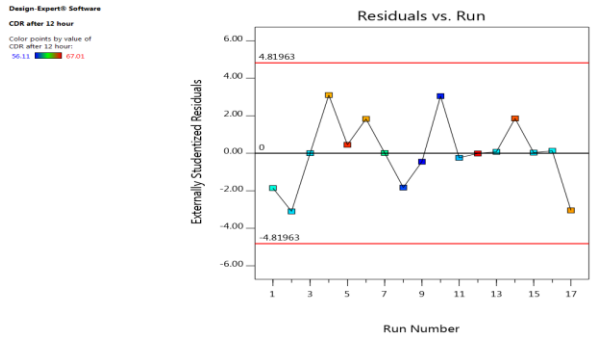

Figure-18: Residuals vs. Run (R4).

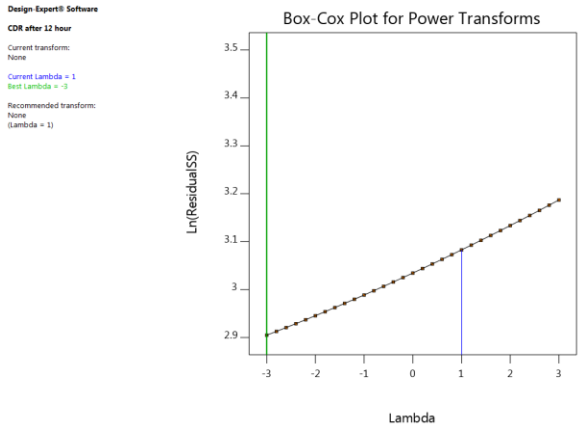

Figure-19: Box-Cox Plot for Power Transforms (R4).

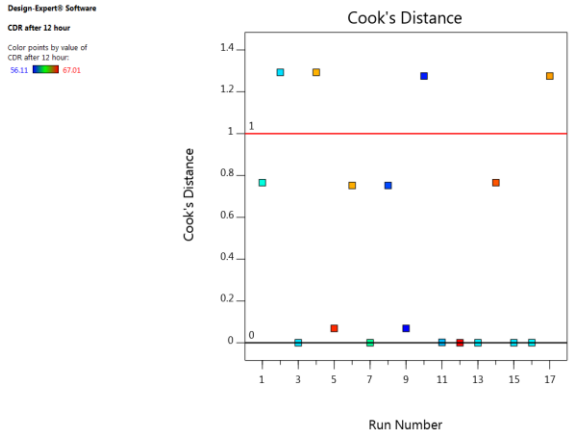

Figure-20: Cook's Distance vs. Run (R4).

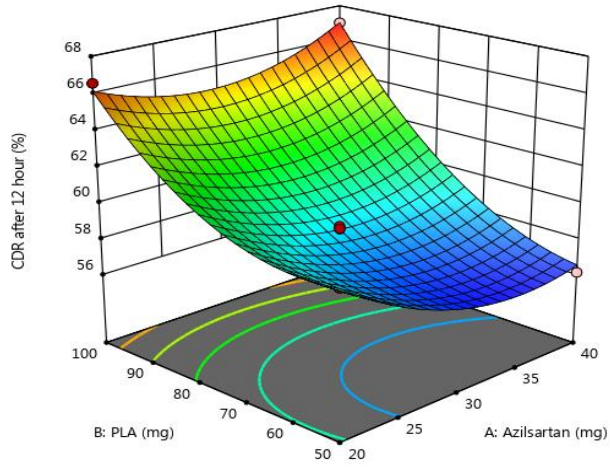

Figure-21: Response surface plot presenting the interaction between the drug and PLA affecting the percentage of cumulative drug release after 12 hour (R4).

The perturbation plot and 2D contour showing the main effects of A, B and C on the particle size (R1), polydispersity index (R2), entrapment efficiency (R3) and percentage of CDR after 12 hour (R4) of azilsartan nanoparticles were shown in the Figure 22 and Figure 23.

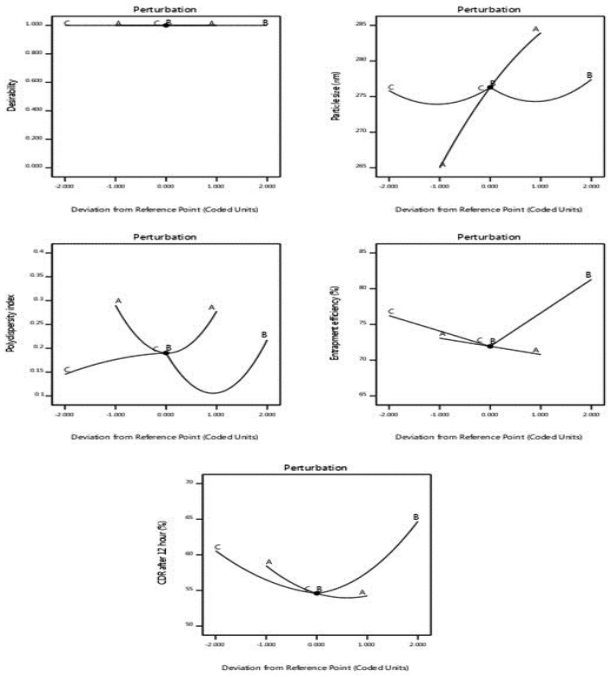

Figure-22: Perturbation plot showing the main effect of Drug (A), PLA (B) and Sonication time (C) on particle size (R1), polydispersity index (R2), entrapment efficiency (R3) and percentage of cumulative drug release after 12 hour (R4).

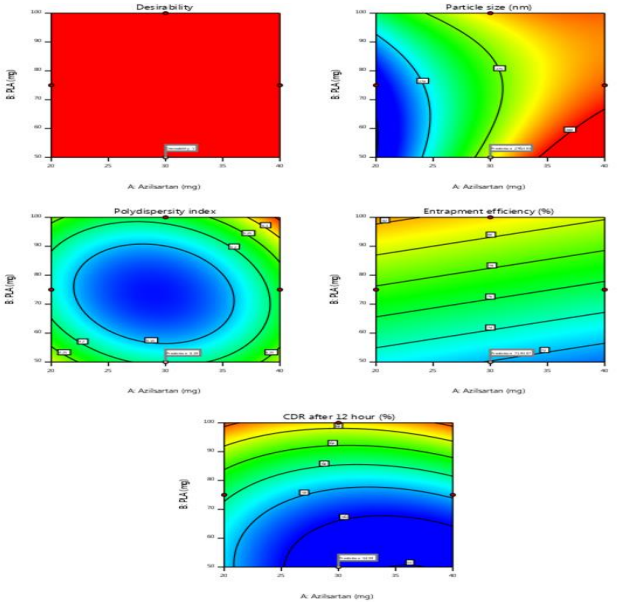

Figure-23: Response surface plot presenting the interaction between the drug and PLA affecting the particle size (R1), polydispersity index (R2), entrapment efficiency (R3) and percentage of cumulative drug release after 12 hour (R4).

The FTIR spectral analysis of azilsartan, pure drug showed the principal peaks were observed at 3929.50, 3882.73, 3838.17, 3760.53, 3666.28, 3544.64, 3437.95, 3216.96, 3006.25, 2782.05, 2560.04, 2440.11, 2289.41, 2198.50, 2089.45, 1942.97, 1915.70, 1831.63, 1735.63, 1563.08, 1435.83, 1281.94, 1160.19, 1045.32, 817.36, 663.44 and 505.68 (unit cm^{-1}). The spectral analysis of pure PLA showed peaks at 3827.31, 3663.04, 3511.87, 3402.17, 3304.50, 3269.88, 3212.63, 3069.03, 2924.03, 2742.09, 2565.15, 2439.66, 2855.99, 2097.66, 1992.87, 1796.59, 1707.61, 1531.39, 1428.89, 1259.15, 1171.89, 1048.06, 858.14, 811.60, 763.56, 674.06, 574.84 (unit cm^{-1}). The spectrum of physical mixture of azilsartan with PLA showed the peaks at 3832.13, 3799.03, 3668.84, 3529.86, 3436.33, 3320.10, 3225.05, 3097.69, 2806.72, 2665.13, 2562.35, 2430.04, 2324.84, 2196.84, 2082.80, 1961.61, 1793.94, 1672.54, 1432.31, 1170.00, 1045.98, 813.10, 759.41, 684.84, 568.57, 476.19 (unit in cm-1). The spectrum of nanoparticle showed peaks at wavenumbers of 3832.01, 3798.86, 3704.33, 3547.29, 3385.03, 3309.40, 3089.53, 2950.76, 2804.12, 2607.95, 2490.93, 2355.26, 2208.95, 2090.01, 1993.18, 1915.83, 1736.35, 1711.09, 1529.92, 1436.31, 1253.96, 1036.54, 845.66, 812.86, 687.52, 568.16 (unit cm^{-1}). The results of the FTIR spectroscopy confirmed the compatibility of drug and polymer. Azilsartan was capable of forming polymeric nanoparticles with PLA without disturbance in the functional groups as shown in Figure 24 a,b,c & d.

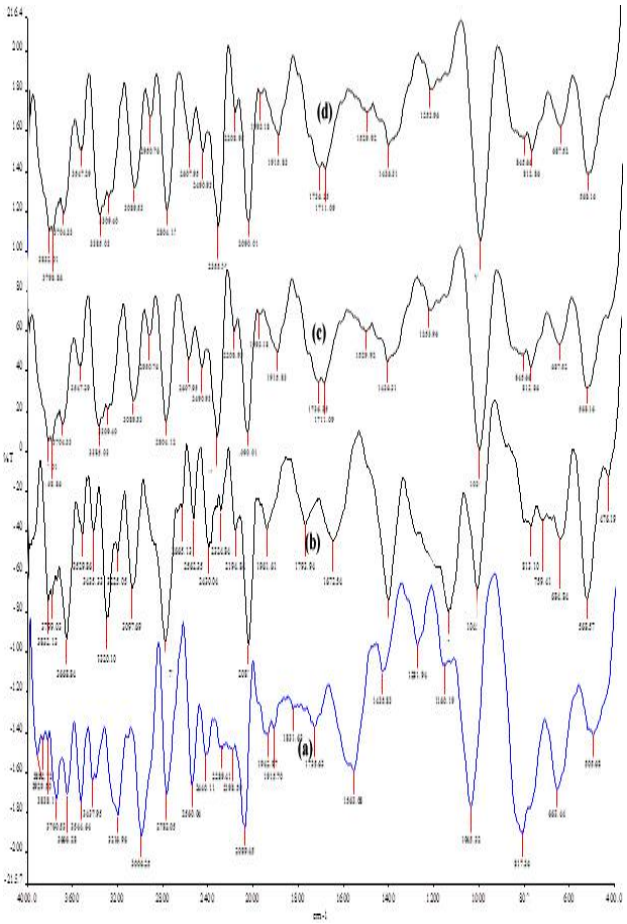

Figure-24: (a) FTIR Spectrum of Azilsartan. (b) FTIR Spectrum of PLA. (c) FTIR Spectrum of physical mixture of azilsartan and PLA. (d) FTIR Spectrum of azilsartan-PLA nanoparticle.

Table-9: Optimized values obtained by the constraints apply on R1, R2, R3 and R4.

Predicted values				Batch	Observed values			
Particle size (R1), nm	Polydis-persity index (R2)	Entrap-ment efficiency (R3), %	CDR after 12 hours (R4), %		Particle size (nm)	Polydis-persity index	Entrap-ment efficiency (%)	CDR after 12 hours (%)
270.71	0.1022	78.7594	58.552	A3	270.71	0.1022	78.7594	58.552
				A15	270.70	0.1022	78.7594	58.560
				A16	270.71	0.1021	78.7594	58.551

The formulation process was optimized to obtain the desired responses. Numerical optimization using the desirability approach was employed to find out the optimal process variables. Optimized conditions were obtained by setting constraints on the dependent and independent variables. A3, A15, A16 batches code of azilsartan nanoparticles were prepared according to optimized levels. The observed values of responses were then compared to the predicted values and were found to be in close agreement with the predicted values of the optimized process, thereby demonstrating the validity of the optimization procedure. The predicted values and observed values of responses were recorded in (Table 9).

Modified emulsification technique produced spherical, relatively smooth surfaced nanoparticles as shown in (Fig. 25). Scanning Electron

Microscope analysis provides visual and descriptive information of a portion of whole population of the sample thus a clear picture of all the particles may not be obtained. Particle size plays an important role in improving the bioavailability of the drug loaded NPs.

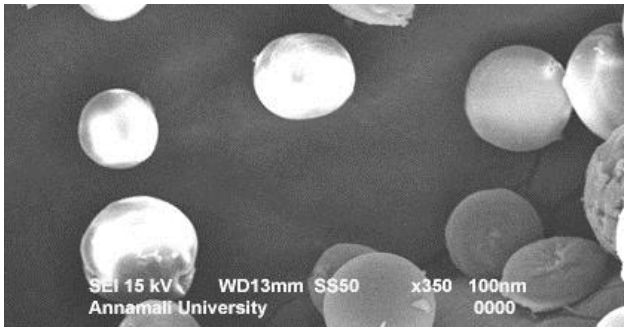

Figure-25: SEM images of Azilsartan nanoparticles.

CONCLUSION

From the study, it can be concluded that azilsartan nanoparticles can be prepared with PLA. The process parameter such as drug concentration, polymer concentration and sonication time were investigated for their effects on particle size, polydispersity index, entrapment efficiency and percentage of cumulative drug release after 12 hours. After that the process parameters were optimized and the observed values for the four responses of optimized formulation were found to be in close agreement with the predicted values by computed models.

REFERENCE

[1] HW Darwish, AH Bakheit, AS Abdelhameed, B Mustafa. A novel method to determine new potent angiotensin inhibitor, azilsartan, in human plasma via micelle-enhanced spectrofluorimetry using cremophor RH 40. *Trop J Pharm Res*.15(5):1003–12(2016).

[2] S Garaga, NC Misra, AV Raghava Reddy, KJ Prabahar, C Takshinamoorthy, PD Sanasi, et al. An alterative synthesis of azilsartan kamedoxomil: An angiotensin II receptor blocker. *Org Process Res Dev*.19(4):514–9(2015).

[3] KS Surwade, RB Saudagar. Solubility enhancement of azilsartan medoxomil using mixed hydrotrophy. *World Journal of Pharmacy and Pharmaceutical Sciences.* 4(7):1167-1179(2015).

[4] B Khera, N Sen, SG Moghe, NS Parhi. Stable pharmaceutical package comprising azilsartan medoxomil. United States Patent Application Publication. Pub. No.: US 2016/0008328 A1. 2016; 1(14).

[5] I Rosenberger, A Strauss, S Dobiasch, C Weis, S Szanyi, L Gil-Iceta, et al. Targeted diagnostic magnetic nanoparticles for medical imaging of pancreatic cancer. *J Control Release*. 214:76–84(2015).

[6] How's that Nanoparticle Biocorona treating you?? The Pipettepen. [Cited 2018 May 13]; Available from: http://www.thepipettepen.com/blog/hows-that-nanoparticle-biocorona-treating-you.

[7] A Krais, L Wortmann, L Hermanns, N Feliu, M Vahter, S Stucky, et al. Targeted uptake of folic acid-functionalized iron oxide nanoparticles by ovarian cancer cells in the presence but not in the absence of serum. *Nanomedicine Nanotechnology*.10(7):1421–31(2014).

[8] A Sabzevari, K Adibkia, H Hashemi, A Hedayatfar, N Mohsenzadeh, F Atyabi, Ghahremani MH, R Dinarvand. Polymeric triamcinolone acetonide nanoparticles as a new alternative in the treatment of uveitis: In vitro and in vivo studies. *European Journal of Pharmaceutics and Biopharmaceutics*. 84: 63–71(2013).

[9] F Rancan, D Papakostas, S Hadam, S Hackbarth, T Delair, C Primard, et al. Investigation of polylactic acid (PLA) nanoparticles as drug delivery systems for local dermatotherapy. *Pharm Res*.26 (8):2027–36(2009).

[10] K Fernández, J Aburto, C Von Plessing, M Rockel, E Aspé. Factorial design optimization and characterization of poly-lactic acid (PLA) nanoparticle formation for the delivery of grape extracts. *Food Chem*.207:75–85(2016).

[11] CM Luz, MSP Boyles, P Falagan-Lotsch, MR Pereira, HR Tutumi, E Oliveira Santos,et al. Poly-lactic acid nanoparticles (PLA-NP) promote physiological modifications in lung epithelial cells and are internalized by clathrin-coated pits and lipid rafts. *J .Nanobiotechnology*.15 (1):1–18(2017).

[12] SH Suhaimi, R Hasham, NA Roslic. Effects of formulation parameters on particle size and polydispersity index of orthosiphon stamineus loaded nanostructured lipid carrier. *Journal of Advanced Research in*

Applied Sciences and Engineering Technology, 1(1): 36-39(2015).

[13] NA Jassem, NA Rajab. Formulation and in vitro evaluation of azilsartan medoxomil nanosuspension. *International Journal of Pharmacy and Pharmaceutical Sciences*.9 (7):110-119 (2017).

[14] A Avinash, A Sushma, K Lalasa, SP Kumae, T Gowthami, M Sreenivasulu. Solubility and Dissolution Rate Enhancement of Olmesartan Medoxomil by Hydrotropy and Development of Oral Disintegrating Tablets. *IJMPR.*4(4): 198-206(2016).

[15] S Kalidoss, K Koumaravelou, A Kottaimuthu. Formulation development and evaluation of colon targeted oral drug delivery system of azilsartan medoxamil. *European Journal of Biomedical and Pharmaceutical sciences.*4 (04):692-699(2017).